Effects of non-linear soil deformation on the response of simple 2-D basins

J. Zhang & J.X. Zhao

Institute of Geological & Nuclear Sciences Limited

2005 NZSEE Conference

ABSTRACT: Nonlinear seismic responses of 2-dimensional (2-D) soft-soil basins, with 3 width/depth ratios and excited by 186 accelerograms (including 78 scaled accelerograms) recorded on rock sites, have been evaluated by using 1-D and 2-D models. The curves of mean 5% damped response spectral acceleration amplification ratio for various spectral periods are presented and are used to evaluate the effects of basins and nonlinear soil response. The mean response spectral amplification ratios for peak ground acceleration (PGA) and other spectral periods are found to vary considerably across a basin and for basins with different width/depth ratios. For spectral periods up to 1.0s, the amplification ratios decrease with an increase of input response spectral acceleration, but are nearly constant for longer spectral periods. For each basin at short spectral period, the crossover points vary considerably at various locations. The input response spectral accelerations at the crossover points for spectral periods larger than 0.2s are larger than those from PGA plots. The 1-D models underestimate the amplification ratios for small input response spectral accelerations and provide an approximation for large input response spectral accelerations at the centres of basins with width/depth ratio 6 or larger. The variation of amplification ratios in a basin under weak excitation does not bear any resemblance to that under moderate or strong excitation.

1 INTRODUCTION

Ground motion in earthquakes is often amplified by soft soil layers (Idriss 1990) and the amplification can lead to significant structural damage as in the cases of Mexico City. Much research has been done in assessing the soil amplification effect. Elastic responses of 2- or 3-dimensional soil basins have been estimated by many researchers, with the emphasis of these studies being mainly on long-duration ground shaking, surface waves induced by the basins and the amplification of peak ground response. Usually, these studies modelled responses of very large basins, with widths and depths of a few kilometres. Due to the limitation of computing power, however, soils with low shear-wave velocities, 150-300m/s, in the surface layers were not modelled. The engineering impacts of such studies are therefore limited because ground-motion amplification by low-velocity surface soil layers is often an important design parameter for engineering structures.

In the present study, an approach similar to those of Zhao et al (1999) and Ni et al (2000) is adopted. Amplification ratios are computed by using 186 accelerograms recorded on engineering rock sites (NEHRP site class, (BSSC 1994)) in earthquakes with varying magnitudes and source distances. A mean response spectral amplification ratio curve is fitted to these amplification ratios by using the least-squares method. The variation of amplification ratio, as a function of input response spectral acceleration for different spectral periods, is estimated and used to assess the effect of basins and nonlinear soil deformation. The limitations of using 1-D models for estimating ground motion responses of 2-D basins are ascertained for different spectral periods by comparing the amplification ratio curves from 1-D and 2-D models. The response spectral amplification ratio curves derived from the present study can also be used to derive probabilistic response spectra for soft soil sites, as shown by Zhao et al (1999), to compensate the limitation for a lack of strong motion data recorded on soft soil basins.

2 BASIN TYPES, MATERIAL MODELS AND ROCK SITE STRONG MOTION DATABASE

We limit the present study to very simple symmetric basins that have a shear wave velocity profile as shown in Figure 1. For all basins, the basin depth is 30m, the shear wave velocity of the soil is 175m/s, and the slope of basin edge is fixed at 45^o. Basin 1 is a narrow basin with a width/depth (W/H) ratio of 3 (W is the total width of the basin on ground surface and H is the depth of the basin), basin 2 has a W/H of 6, and basin 3 has a W/H of 10. Four stations (see Fig. 1) are labelled as A at the middle of the sloped basin edge, B at the corner of the basin edge, C at the quarter width of the basin bottom and D at the centre of the basin. The fundamental periods for the stations are 0.42s for station A and 0.76s for stations B to D.

On the two vertical and the horizontal bottom boundaries of the basin model, energy transmitting boundaries (viscous dashpots) are located. A very simple nonlinear soil model, hyperbolic model, is used in the present study and is described as,

$$\frac{G}{G_{\max}} = \frac{1}{1+\gamma\, G_{\max}/\tau_{\max}} \qquad (1)$$

where $G = \tau/\gamma$ is the secant shear modulus, τ_{max} is the soil shear strength and taken as $73.9kP_a$, G_{max} is the maximum shear modulus at small shear strain, and $G_{max}=\rho V_s^2$, where ρ is the soil mass density and taken as $18kN/m^3$ and V_s is the soil shear wave velocity at small shear strain.

Horizontal components of rock site records from the 1989 Loma Prieta earthquake (M_w=6.9) and the 1994 Northridge earthquake (M_w=6.7) were selected as excitations for the models, which were recorded on engineering rock sites. To show the effect of various earthquake events, records from several European, Japan, and American strong earthquake events were also added to the database. Due to the limited amount of data, part of selected records with PGA less than 0.01g were scaled by a factor of 0.2 to represent ground motions either at a remote site from a large event or a short distance from a small event, and some with PGA greater than 0.2g were scaled by a factor of 2 to represent strong ground motions from very large earthquakes, although we know that errors for the duration exist.

3 AMPLIFICATION OF PEAK GROUND ACCELERATIONS

Amplification of peak ground acceleration (PGA) for soil sites has been used widely to gauge the effect of nonlinear soil response. The amplification curves most cited are those from Idriss (1990), where PGA ratios adjacent rock and soil sites are plotted to show that soil site PGAs are amplified at small rock site PGAs while they are deamplified at large rock site PGAs. A crossover point, where the amplification ratio is equal to 1, is used to separate amplification and deamplification. In the study of Idriss, only limited data were available from the 1989 Loma Pretia earthquake, and most data with large PGAs were from 1-D modelling of site response with the SHAKE program, using an equivalent linear method to approximate the nonlinear soil response.

To explore the effects of nonlinear soil response and basin geometry on ground response, the estimated PGA amplifications for 4 stations of the simple 2-D basins (A, B, C and D in Fig. 1) are presented based on amplification ratio in this Section. Because there is a considerable amount of scatter as a result of the differing spectral shapes (Zhao et al, 1999) for different input motions, Equation 1 is used to fit a smoothed amplification curve as following:

$$\ln(SR) = a \ln[\, b\,(PGA_{rock})^c + d\,] \qquad (2)$$

where SR denotes the response spectral amplification ratio, PGA_{rock} is the input PGA value, and a, b, c and d are constants determined by regression analysis.

Comparisons of computed amplification ratios and fitted mean amplification curves are shown in Figures 2a and 2b for basin 2 (with W/H of 6). Station A has larger scatter than station D for large excitation level. A possible reason may be that the contribution from higher modes of the basin at station A is larger than that at station D where the first mode

dominates the ground response. For excitation PGAs less than 0.25g, the amplification at station A is less than that at station D, but above 0.25g, the amplification at station A is larger than that at station D, showing that strong nonlinear soil response reduces soft soil amplification at the basin centre. The excitation PGA at the crossover point is 1g for station A and close to 0.37g for station D. In the present study, the range of the used earthquake records is considered to be large enough to reveal the trend of the amplification ratio reduction with increasing excitation PGA, although for station A there is no data above the rock site PGA at the crossover point. Note that there is little difference in the PGA amplification ratios between the data from the 1989 Loma Prieta event, the 1994 Northridge event, and the Japanese crustal events.

Amplification curves from the 2-D models at stations A, B, C, and D and from the 1-D models at stations A and D for basin 2 (with W/H of 6) are shown in Figure 3. At small excitation levels, the amplification ratios gradually increase from stations A to D, while at larger excitation levels they gradually decrease from stations A to D. PGAs at crossover points for stations A and B are 1.0g and 0.65g, and for stations C and D are about 0.37g, suggesting that the PGA at cross-over points depend not only on the nonlinear soil response, but also on the basin effects. Relative to the PGA range of 0.3g to 0.4g for crossover points of Idriss (1990), stations A and B have much larger PGA values and stations C and D have similar PGA values, indicating, as known, that basin effects on ground response are more significant near the basin edge than at the basin centre, even when the nonlinear response of the soil is strong. Figure 3 also shows that at excitation levels up to 0.01g, the reduction in amplification ratio with increasing PGA is small. This is because the amplification ratio for excitation PGA of less than 0.01g is primarily controlled by energy leakage (with negligible hysteretic damping), although the energy leakage effect is only moderate for PGAs.

Amplification ratios for two 1-D models for stations A and D in Figure 3 show little difference for PGA up to about 0.1g. Beyond 0.1g, the 1-D model for station D shows stronger amplification reduction with increasing excitation PGA than station A, presumably due to strong nonlinear soil response (the 1-D models for stations A and D differ only in the soil layer thickness). At an excitation PGA less than 0.02g, amplification ratios from the 1-D models are lower than those from the 2-D models, and for excitation PGAs beyond 0.2g, the amplification ratio of the 1-D model for station D is close to those of stations C and D of the 2-D model and is much lower than that at station B. In contrast, the amplification ratio of the 1-D model for station A is close to that of the 2-D model only in a range of 0.02-0.4g for excitation PGA and is much lower than that of the 2-D model for PGA out of the range. The excitation PGA at the crossover point for station D from the 1-D model is close to those of stations C and D from the 2-D model, but for station A is less than that of the 2-D model.

The effect of basins with different W/H ratios on the ground response at stations A to D is shown in Figure 4. For stations A and D at weak and strong excitations, the amplification is quite different (see Fig. 4a). For station A, the amplification ratios for the 3 basins at small excitation levels differ greatly, and the differences decrease gradually with increasing excitation levels. For station D, the differences of the amplification ratios for the 3 basins are small at small excitation levels and large at large excitation levels. These results indicate that the behaviour of near-edge sites differs from that of near-middle sites. PGAs at crossover points for station D of the 3 basins are about 0.75g for basin 1, 0.37g for basin 2, and 0.34g for basin 3. For station D, Figure 4a shows that the 1-D model predicts similar amplification ratios for basins 2 and 3 for excitation PGAs over 0.2g and under-predicts amplification up to 0.2g while prediction from the 1-D model for station A are different from those from the 2-D models except for excitation PGAs less than 0.2g for basin3. Note that the relative amplification ratios between the 3 basins at large excitation PGAs (over 0.2g) do not resemble those from small excitation PGAs.

Figure 4b shows the amplification ratios for stations B and C of all 3 basins. Comparison of Figure 4a and 4b shows: 1) the variation of amplification ratios with respect to excitation PGA at stations B and C are reasonably similar to those at stations A and D, respectively, and

PGAs at crossover points for stations B and C lie between those of stations A and D, and 2) the 1-D model predicts very similar amplification ratios for station C of basins 2 and 3 at excitation PGAs over 0.1g while it predicts much smaller amplification ratios at small excitation PGAs than the 2-D models, and the 1-D model significantly under-predicts the amplification of the 2-D model at station B for all 3 basins. Note again that the amplification ratios for weak shaking differ considerably from those for strong shaking.

4 AMPLIFICATION OF SPECTRAL ACCELERATIONS

Because of period-dependent features, the variation of the response spectral amplification ratio with respect to the input spectral acceleration for a given spectral period is more complicated than the variation of PGA amplification ratio. In order to compare the mean amplification ratios between different stations and different basins, a continuous amplification curve is fitted to the computed amplification ratios. The following equations are used:

$$\ln[SR(T)] = \begin{cases} a\ln\{b[SA_{rock}(T)]^c + d\} & for\ T \le T_c \\ a\ln\{b[SA_{rock}(T_c)]^c + d\} + f\{\ln(SA_{rock}(T)] - \ln[SA_{rock}(T_c)]\} & for\ T > T_c \end{cases} \quad (2)$$

and alternatively

$$\ln[SR(T)] = \begin{cases} a\ln[SA_{rock}(T)] & for\ T < T_c \\ a\ln[SA_{rock}(T_c)] + f(\ln\{b[SA_{rock}(T)]^c + d\} - \ln\{b[SA_{rock}(T_c)]^c + d\}) & for\ T \ge T_c \end{cases} \quad (3)$$

where *SR(T)* and $SA_{rock}(T)$ are the response spectral amplification ratio and the input spectral acceleration for a given spectral period, respectively, T_c is the period of the interception of the two curves if two segments are used, and coefficients a, b, c, d, and f are constants derived from regression analysis. Note that for the purpose of best fitting the computed amplification ratios, two function forms are provided. In the present study, we attempt to fit the computed data as closely as possible without any restraint on the parameters arising from possible links to the physical soil properties.

Figure 5 shows the fitted amplification curves and the computed data for stations A and D for basin 2 (W/H=6) at 0.2s spectral period with the scatter being similar to that for PGA (Fig. 2). The standard errors of the fitting for stations A and D are very similar, about 0.24. The input spectral accelerations at crossover points are 2g and 0.8g, compared to 1g and 0.37g in Figure 2 (PGA plot). The mean amplification ratios of the two stations have a nearly linear amplification reduction (using a natural logarithm scale) with the increase of input spectral acceleration, but the range of the linear reduction at station A is much larger than that at station D. Note that there is no input spectral acceleration below 0.01g, and so the amplification at small excitation levels is not well restrained. In the following parts, all comparisons are based on the mean amplification ratios derived from Equations 3 or 4.

Two spectral periods of 0.5s and 2.0s are chosen to show the effects of nonlinear soil response for basin 2 (W/H=6), as shown in Figures 6a and 6b. For 0.5s spectral period in Figure 6a, the effect of nonlinear soil response is the largest at station D and smallest at station A based on the rate of the amplification ratio reduction with increasing excitation level. Input spectral accelerations at crossover points for stations A to D are about 2.0g, 1.1g, 1.1g and 0.58g, respectively, and are larger than those for PGA in Figure 3 (PGA plot). Note that at large excitation levels the amplification ratios for stations B and C are similar, but different from those in Figure 3 where the amplification ratios for stations C and D are similar. Figure 6a also shows the mean amplification curves of the 1-D models for stations A and D. The 1-D models provide a poor prediction for the amplification ratio of the 2-D basin for nearly all excitation levels for stations A to C, except that the 1-D model provides a good approximation for the amplification ratio of the 2-D basin at station D at large excitation level.

Figure 6b shows the curves of mean amplification ratios for stations A to D at 2.0s spectral period for basin 2 (with W/H of 6), together with those of the 1-D models. Different from those in Figures 3 and 6a, the amplification ratios lie in the range of 1.0 to 2.0 for most input

spectral accelerations. Rodriguez-Marek et al (2001) also derived a similar result from their empirical analyses for the amplification ratio of site D with respect to site B, but our study focuses on the amplification ratio of site E with respect to sites A/B. Figure 6b also shows that the effect of nonlinear soil response is not significant (due to the small amplification ratio reduction rate with respect to input spectral acceleration), but basin effect is significant because the amplitudes of the amplification ratios at the four stations are quite different. It is worth noting from Figure 6b that the amplification ratios predicted by the two 1-D models have the same order as those predicted by the 2-D models, but the difference from amplitudes of amplification ratios exists for any station.

Our results show that the reduction of amplification ratios generally decreases with increasing period, suggesting that the effect of nonlinear soil response reduces with increasing periods. This is presumably because the long wave length of the long period ground motions results in smaller shear strain in the soil than the short period ground motions with the short wave length even if the amplitudes of the long and short period ground motions are similar. Also for 1.0s spectral period, a constant amplification ratio is in the range of input spectral accelerations up to 0.1g and nearly constant for all levels of excitation for 2s spectral period. For all periods, the amplification ratios do not vary with increasing excitation in a "regular or systematic" manner (see Fig. 6a) and this is probably a result of complicated interaction between the dominant period shift, energy leakage and energy dissipation due to nonlinear soil response. The predictions from the 1-D and 2-D models are more different for a short spectral period than for a long spectral period, and for a given spectral period, the difference is clearer for small input spectral accelerations than for large input spectral accelerations.

5 VARIABILITY OF AMPLIFICATION RATIOS

The standard error of fitted curves to the computed amplification ratios is also an important parameter because it affects the estimated probabilistic design spectra for soft soil sites (Zhao et al 1999). The variability was accounted for by Zhao et al (1999) by simply adding a factored standard deviation to the mean probabilistic response spectra for the soil site of interest, in that variability was produced only from nonlinear 1-D models. In the present study, variability produced by basins and soil nonlinearity are considered.

Table 1 shows the standard errors for fitting the computed amplification ratios of the 1-D models and the 2-D models, for PGA and spectral acceleration at periods of 0.2s, 0.5s, 1.0s and 2.0s. The standard errors are given as natural logarithms. To estimate the 84 percentile spectral ratio, the mean spectral ratio can be multiplied by the exponent of one standard error given in Table 1.

For the 1-D model for station A, the PGA amplification ratio has the largest standard error of 0.193 and the smallest standard error is for 2s spectral period, only 0.115. The standard errors of the 1-D model for station D are between 0.137 and 0.169. These values are similar to those reported by Zhao et al (1999). For stations B, C and D of the 2-D models, the standard errors for PGA are smaller than those for most spectral periods. The reason for this is because the spectral accelerations consistent with the crossover points for PGA are lower than those for most spectral periods and as well known that strong nonlinear soil response reduces the scatter of amplification ratios. For PGA of the 2-D models, station A has the largest standard error while station D has the smallest standard error, except for basin 2 for which station C has the smallest standard error. For spectral periods up to 2.0s, station A of basins 2 and 3 have smaller standard errors than basin 1. Standard errors appear to decrease with increasing spectral period for station A, and the standard errors for PGA at stations C and D are considerably smaller than for the other periods. The largest standard error results a factor of 1.25 which is not large compared with the other uncertainties common in estimating response spectra from empirical models. Note that it is likely that basin has little effects on standard deviations of amplification ratio, but soil nonlinearity does.

6 CONCLUSIONS

The following conclusions can be reached from the present study:

1) The rate of amplification ratio reduction of peak ground accelerations (PGA) with respect to excitation PGA for the 2-D soft-soil basin varies across the basin. The excitation PGA at the crossover point (beyond which deamplification occurs) varies with locations on ground surface and with width/depth (W/H) ratios of basins. At the centre of basins with a ratio of W/H larger than 6, the excitation PGAs at the crossover points are close to those of Idriss (1990), but there are great differences at stations near the edges of basins; 2) 1-D models generally underestimate the amplification ratio of a 2-D basin at weak to moderate excitation levels for PGA and various spectral periods. For basins with W/H=6 and 10, the 1-D model predicts the amplification ratio reasonably well for stations at the centre of the 2-D basins at strong excitation only; 3) for spectral periods up to 1s, amplification ratios decrease with increasing excitation level. The input spectral accelerations at the crossover points for the discussed spectral periods are larger than those derived from PGA plot. Due to basin effects, the input spectral accelerations at crossover points are usually smaller for wide basins than for narrow basins. As spectral periods increase, the input spectral accelerations at crossover points also increase, and when spectral period is up to 2.0s, no deamplification occurs again. 4) the variability of amplification ratios is reasonably small, typically within a factor of 1.25 which is much smaller than the variability in estimating spectra of strong ground motions from empirical attenuation models. The variability could be reduced by soil nonlinear response, and basin effects for the variability are small.

REFERENCES:

BSSC, 1994, NEHRP recommended provisions for seismic regulations for new buildings, Part I - Provisions, *FEMA 222A, Federal Emergency Management Agency, 290pp.*

Idriss, I.M. 1990. Response of soft soil sites during earthquakes, *In: Proc. Memorial Symp. to honour Professor Harry Bolton Seed, Vol.(II) 273-289,* Berkeley California,.

Ni, S.D Anderson, J.G. Zeng, Y. &Siddharthan, R.V. 2000, *Expected signature of nonlinearity on regression for strong ground-motion parameters*, Bulletin of Seism Soc of America, 2000;90(6B): 53-64..

Rodriguez-Marek, A. Bray, J.D. Abrahamson, N.A. 2001 *An empirically based geotechnical seismic site response precedure*, Earthquake Spectra, 17(1) 65-87.

Zhao, J.X. Davenport, P.N. McVerry, G.H. 1999 *Modelling and earthquake response of Gisborne Post Office site*, *New Zealand*, Bulletin of the New Zealand Society for Earthquake Engineering, 32(3) 146-169.

Table 1 Standard errors of 1-D and 2-D models

Period (s)	Station				Station				Station				Station	
	A	B	C	D	A	B	C	D	A	B	C	D	A	D
	Basin 1 W/H=3				Basin 2 W/H=6				Basin 3 W/H=10				1-D	
PGA	0.23	0.16	0.15	0.13	0.21	0.18	0.14	0.16	0.20	0.17	0.16	0.15	0.19	0.17
0.2	0.24	0.20	0.17	0.21	0.23	0.20	0.21	0.24	0.23	0.21	0.18	0.18	0.15	0.16
0.5	0.17	0.18	0.18	0.18	0.18	0.19	0.18	0.22	0.15	0.17	0.22	0.18	0.17	0.14
1.0	0.14	0.16	0.20	0.23	0.14	0.16	0.20	0.23	0.14	0.15	0.21	0.24	0.18	0.16
2.0	0.14	0.18	0.22	0.23	0.14	0.18	0.22	0.23	0.13	0.17	0.21	0.21	0.12	0.16

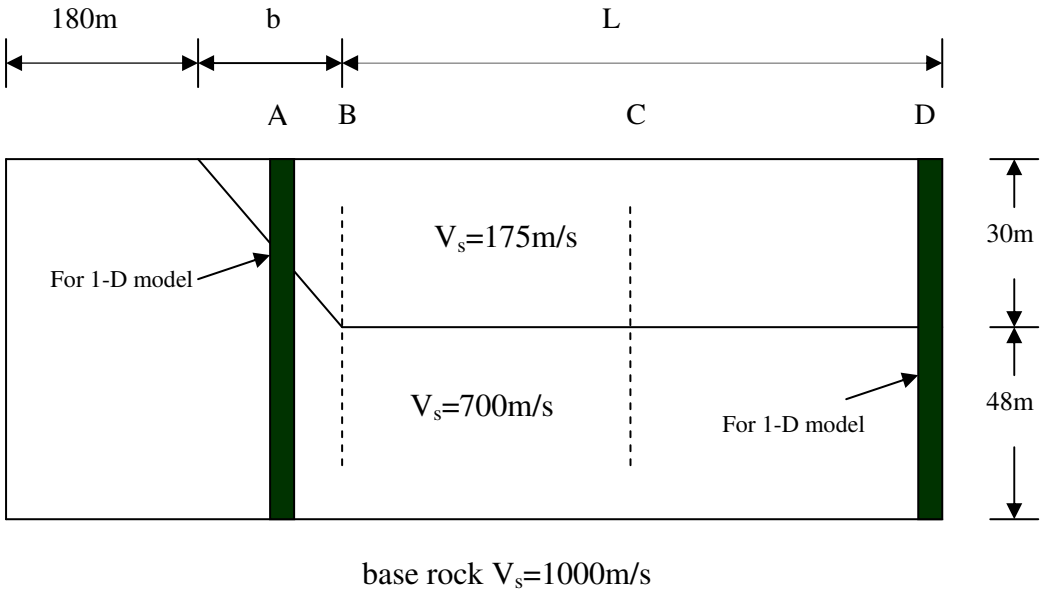

Figure 1 Sketch of basins with the locations of 1-D models and shear wave velocity profile

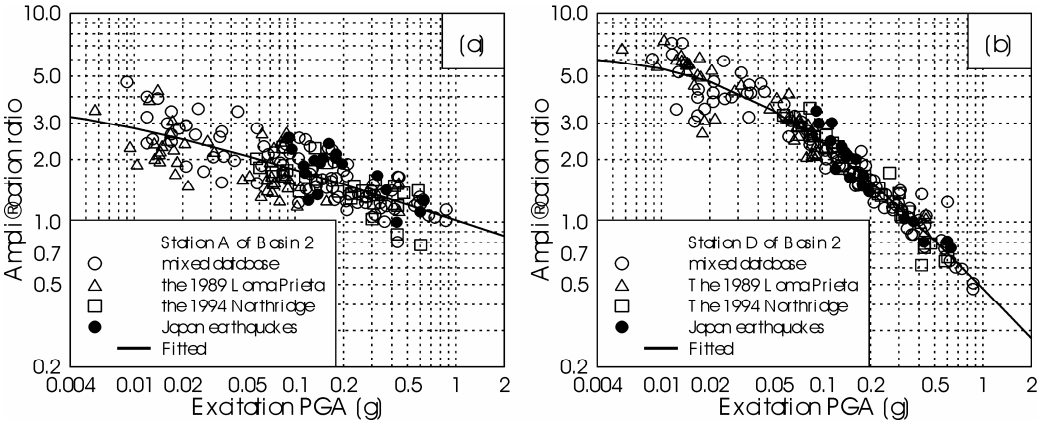

Figure 2 Fitted curves for PGA amplification ratios for basin 2 (W/H=6): (a) at station A, and (b) at station D (basin centre).

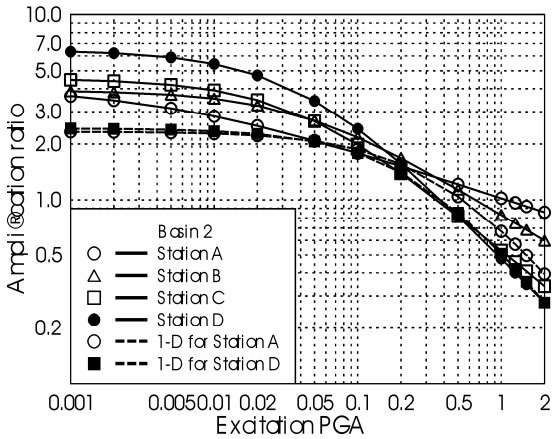

Figure 3 Comparison of PGA amplification ratios at stations A, B, C, and D, together with PGA amplification ratios from 1-D models at stations A and D.

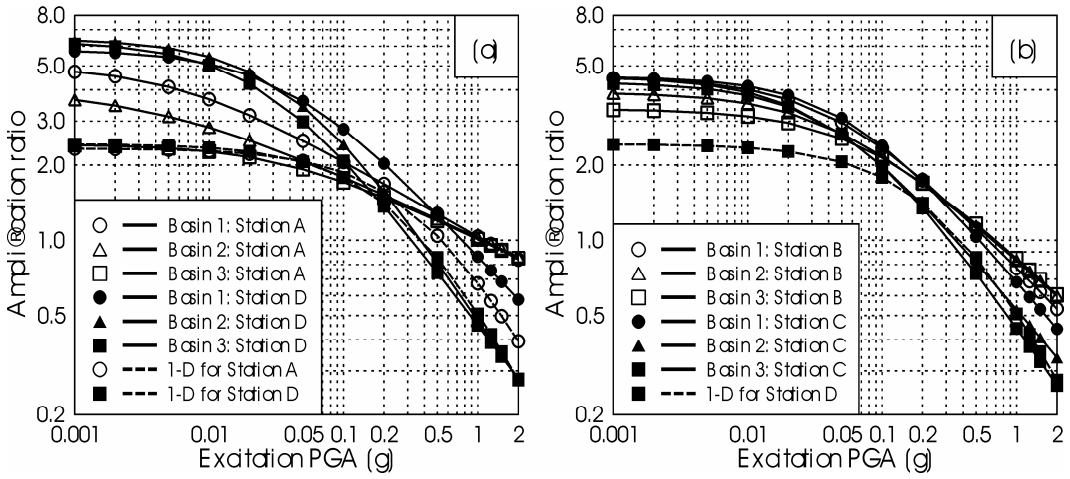

Figure 4 PGA amplification ratios from the 3 basins at stations A, B, C and D, together with PGA amplification ratios from 1-D models at stations A and D.

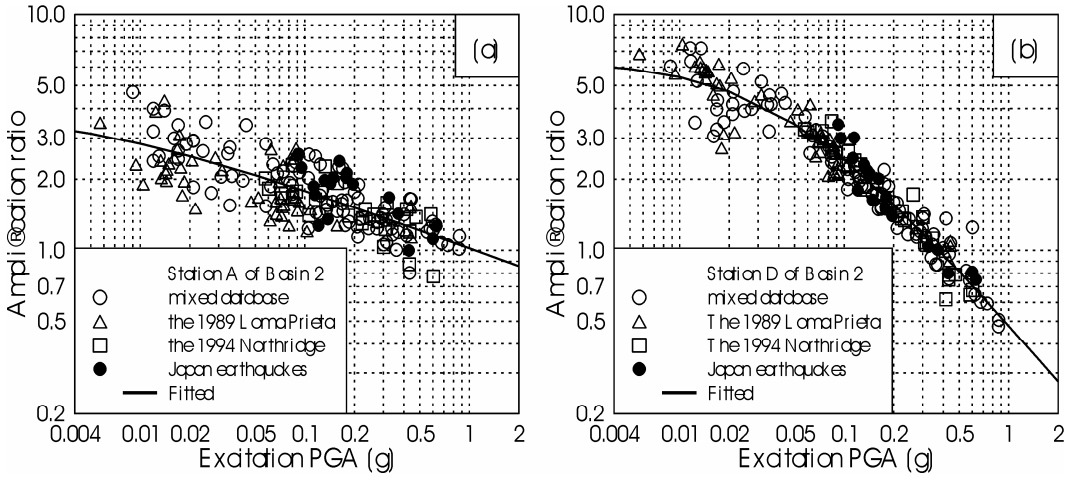

Figure 5 Fitted curves for basin 2 at 0.2s spectral period. (a) at station A and (b) at station D.

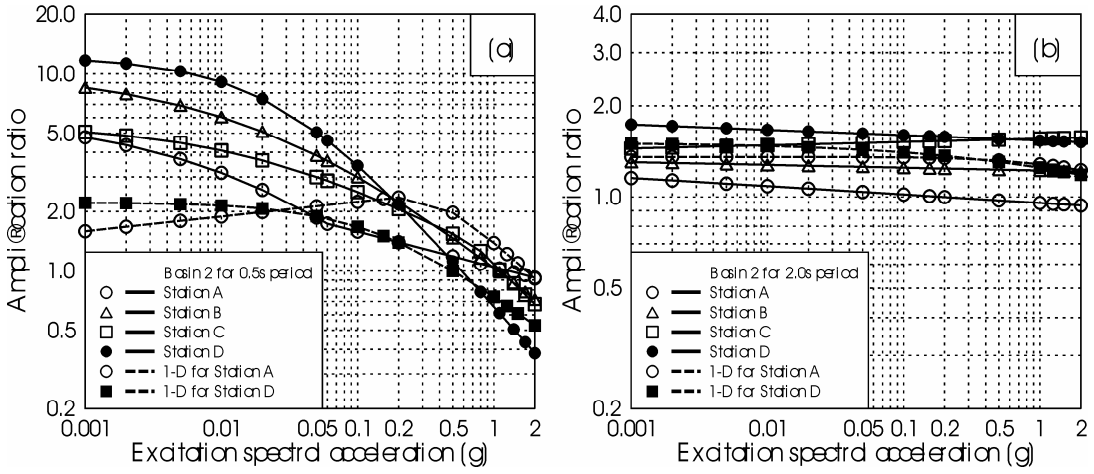

Figure 6 Comparison of spectral amplification ratios for basin 2 at stations A, B, C and D.